Supplementary information for : Decoupling Thermoelectric Parameters in Novel Ionic Layered Materials: A Charged Monolayer Stabilization Strategy for Enhanced Anisotropy

Yaobo Li[‖],[1] Meng Pei[‖],[1] Ziyang Zuo,[2] Dangdang Xu,[1] Zhenzhen Feng,[2] David B. Hayrapetyan,[3] Christos S. Garoufalis,[4,1] Sotirios Baskoutas,[4,1] Yuli Yan,[2,*] and Zaiping Zeng[1,†]

[1] *Henan International Joint Laboratory of Quantum Dot Materials and School of Nanoscience and Materials Engineering, Henan University, Kaifeng, Henan 475001, China*
[2] *Institute for Computational Materials Science, School of Physics and Electronics, Henan University, Kaifeng, Henan 475001, China*
[3] *Institute of Chemical Physics after A.B. Nalbandyan of NAS RA, 5/2 Paruyr Sevak St., Yerevan 0014, Armenia*
[4] *Materials Science Department, University of Patras, 26504 Patras, Greece*

(Dated: February 9, 2026)

* yanyl@henu.edu.cn
† zaiping.zeng@henu.edu.cn

TABLE S1. Formation energies E_f (in unit of eV/atom) and hull distance ΔE_{HD} (in unit of eV/atom) for 64 $\mathrm{LiC^{II}A^{V}}$, $\mathrm{NaC^{II}A^{V}}$ and $\mathrm{KC^{II}A^{V}}$ ternary compounds with crystal structure of Figure 1(d(iv)) in the main text. All the calculations are performed using DFT/PBE level of theory. Those compounds with positive formation energies are underlined.

Materials	E_f (eV/atom)	ΔE_{HD} (eV/atom)	Materials	E_f (eV/atom)	ΔE_{HD} (eV/atom)
LiBeN	-0.875	0.072	NaMgAs	-0.641	0.042
LiBeP	-0.540	0.129	NaMgSb	-0.499	0.058
LiBeAs	-0.437	0.051	NaMgBi	-0.363	0.091
LiBeSb	-0.150	0.142	NaCaN	-0.102	0.435
LiBeBi	0.063	0.321	NaCaP	-0.798	0.147
LiMgN	-0.559	0.167	NaCaAs	-0.846	0.060
LiMgP	-0.744	0.112	NaCaSb	-0.762	0.064
LiMgAs	-0.733	0.023	NaCaBi	-0.639	0.084
LiMgSb	-0.556	0.016	NaSrN	-0.069	0.373
LiMgBi	-0.403	0.028	NaSrP	-0.704	0.220
LiCaN	-0.099	0.633	NaSrAs	-0.774	0.141
LiCaP	-0.826	0.305	NaSrSb	-0.731	0.148
LiCaAs	-0.863	0.210	NaSrBi	-0.623	0.161
LiCaSb	-0.762	0.195	NaBaN	0.110	0.499
LiCaBi	-0.632	0.195	NaBaP	-0.607	0.288
LiSrN	-0.088	0.483	NaBaAs	-0.695	0.209
LiSrP	-0.695	0.373	NaBaSb	-0.683	0.216
LiSrAs	-0.758	0.276	NaBaBi	-0.591	0.224
LiSrSb	-0.705	0.261	KBeN	0.205	0.892
LiSrBi	-0.593	0.255	KBeP	-0.050	0.498
LiBaN	0.129	0.602	KBeAs	-0.039	0.382
LiBaP	-0.575	0.422	KBeSb	0.106	0.401
LiBaAs	-0.658	0.329	KBeBi	0.255	0.502
LiBaSb	-0.639	0.312	KMgN	-0.094	0.429
LiBaBi	-0.544	0.309	KMgP	-0.532	0.209
NaBeN	-0.345	0.368	KMgAs	-0.566	0.128
NaBeP	-0.286	0.296	KMgSb	-0.466	0.131
NaBeAs	-0.231	0.202	KMgBi	-0.346	0.149
NaBeSb	-0.016	0.243	KCaN	-0.191	0.348
NaBeBi	0.162	0.406	KCaP	-0.785	0.099
NaMgN	-0.336	0.186	KCaAs	-0.846	0.019
NaMgP	-0.630	0.115	KCaSb	-0.788	0.023

TABLE S2. Formation energies E_f (in unit of eV/atom) and hull distance ΔE_{HD} (in unit of eV/atom) for 61 $KC^{II}A^{V}$, $RbC^{II}A^{V}$ and $CsC^{II}A^{V}$ ternary compounds with crystal structure of Figure 1(d(iv)) in the main text. All the calculations are performed using DFT/PBE level of theory. Those compounds with positive formation energies are underlined.

Materials	E_f (eV/atom)	ΔE_{HD} (eV/atom)	Materials	E_f (eV/atom)	ΔE_{HD} (eV/atom)
KCaBi	-0.672	0.044	RbBaN	<u>0.142</u>	0.514
KSrN	-0.029	0.392	RbBaP	-0.641	0.110
KSrP	-0.729	0.090	RbBaAs	-0.741	0.027
KSrAs	-0.809	0.010	RbBaSb	-0.752	0.025
KSrSb	-0.786	0.012	RbBaBi	-0.664	0.039
KSrBi	-0.683	0.028	CsBeN	<u>0.933</u>	1.621
KBaN	<u>0.104</u>	0.475	CsBeP	<u>0.245</u>	0.780
KBaP	-0.660	0.109	CsBeAs	<u>0.194</u>	0.615
KBaAs	-0.755	0.028	CsBeSb	<u>0.251</u>	0.562
KBaSb	-0.759	0.043	CsBeBi	<u>0.369</u>	0.634
KBaBi	-0.669	0.062	CsMgN	<u>0.264</u>	0.788
RbBeN	<u>0.550</u>	1.236	CsMgP	-0.386	0.321
RbBeP	<u>0.096</u>	0.627	CsMgAs	-0.445	0.222
RbBeAs	<u>0.084</u>	0.493	CsMgSb	-0.387	0.199
RbBeSb	<u>0.190</u>	0.479	CsMgBi	-0.281	0.209
RbBeBi	<u>0.324</u>	0.564	CsCaN	-0.030	0.509
RbMgN	<u>0.073</u>	0.595	CsCaP	-0.714	0.169
RbMgP	-0.452	0.255	CsCaAs	-0.787	0.086
RbMgAs	-0.497	0.168	CsCaSb	-0.749	0.088
RbMgSb	-0.417	0.163	CsCaBi	-0.125	0.619
RbMgBi	-0.303	0.177	CsSrN	<u>0.066</u>	0.487
RbCaN	-0.105	0.432	CsSrP	-0.688	0.117
RbCaP	-0.740	0.134	CsSrAs	-0.777	0.034
RbCaAs	-0.807	0.062	CsSrSb	-0.769	0.037
RbCaSb	-0.760	0.055	CsSrBi	-0.672	0.053
RbCaBi	-0.648	0.073	CsBaN	<u>0.156</u>	0.527
RbSrN	<u>0.028</u>	0.449	CsBaP	-0.642	0.109
RbSrP	-0.695	0.089	CsBaAs	-0.745	0.026
RbSrAs	-0.783	0.006	CsBaSb	-0.761	0.027
RbSrSb	-0.768	0.014	CsBaBi	-0.676	0.039
RbSrBi	-0.669	0.028			

TABLE S3. Formation energies E_f (in unit of eV/atom) and hull distance ΔE_{HD} (in unit of eV/atom) for 64 $\mathrm{LiC^{II}A^{V}}$, $\mathrm{NaC^{II}A^{V}}$ and $\mathrm{KC^{II}A^{V}}$ ternary compounds with crystal structure of Figure 1(d(v)) in the main text. All the calculations are performed using DFT/PBE level of theory. Those compounds with positive formation energies are underlined.

Materials	E_f (eV/atom)	ΔE_{HD} (eV/atom)	Materials	E_f (eV/atom)	ΔE_{HD} (eV/atom)
LiBeN	-0.863	0.084	NaMgAs	-0.644	0.039
LiBeP	-0.588	0.081	NaMgSb	-0.518	0.039
LiBeAs	-0.489	-0.001	NaMgBi	-0.413	0.041
LiBeSb	-0.205	0.087	NaCaN	-0.296	0.241
LiBeBi	-0.039	0.219	NaCaP	-0.707	0.238
LiMgN	-0.502	0.224	NaCaAs	-0.758	0.148
LiMgP	-0.634	0.222	NaCaSb	-0.678	0.148
LiMgAs	-0.640	0.116	NaCaBi	-0.583	0.140
LiMgSb	-0.493	0.079	NaSrN	-0.121	0.321
LiMgBi	-0.384	0.047	NaSrP	-0.634	0.290
LiCaN	-0.527	0.205	NaSrAs	-0.699	0.216
LiCaP	-0.779	0.352	NaSrSb	-0.613	0.266
LiCaAs	-0.796	0.277	NaSrBi	-0.528	0.256
LiCaSb	-0.605	0.352	NaBaN	<u>0.022</u>	0.411
LiCaBi	-0.505	0.322	NaBaP	-0.579	0.316
LiSrN	-0.383	0.188	NaBaAs	-0.661	0.243
LiSrP	-0.748	0.323	NaBaSb	-0.621	0.278
LiSrAs	-0.785	0.249	NaBaBi	-0.468	0.347
LiSrSb	-0.666	0.300	KBeN	-0.451	0.236
LiSrBi	-0.556	0.292	KBeP	-0.385	0.163
LiBaN	-0.254	0.177	KBeAs	-0.340	0.081
LiBaP	-0.702	0.288	KBeSb	-0.151	0.144
LiBaAs	-0.764	0.223	KBeBi	-0.005	0.242
LiBaSb	-0.676	0.275	KMgN	-0.215	0.308
LiBaBi	-0.576	0.277	KMgP	-0.655	0.086
NaBeN	-0.553	0.160	KMgAs	-0.690	0.004
NaBeP	-0.449	0.133	KMgSb	-0.593	0.004
NaBeAs	-0.383	0.050	KMgBi	-0.491	0.004
NaBeSb	-0.146	0.113	KCaN	-0.229	0.310
NaBeBi	<u>0.013</u>	0.257	KCaP	-0.792	0.092
NaMgN	-0.321	0.201	KCaAs	-0.856	0.009
NaMgP	-0.623	0.122	KCaSb	-0.802	0.009

TABLE S4. Formation energies E_f (in unit of eV/atom) and hull distance ΔE_{HD} (in unit of eV/atom) for 61 $KC^{II}A^{V}$, $RbC^{II}A^{V}$ and $CsC^{II}A^{V}$ ternary compounds with crystal structure of Figure 1(d(v)) in the main text. All the calculations are performed using DFT/PBE level of theory. Those compounds with positive formation energies are underlined.

Materials	E_f (eV/atom)	ΔE_{HD} (eV/atom)	Materials	E_f (eV/atom)	ΔE_{HD} (eV/atom)
KCaBi	-0.707	0.009	RbBaN	<u>0.093</u>	0.465
KSrN	-0.066	0.355	RbBaP	-0.614	0.137
KSrP	-0.699	0.120	RbBaAs	-0.713	0.055
KSrAs	-0.779	0.040	RbBaSb	-0.718	0.059
KSrSb	-0.755	0.043	RbBaBi	-0.646	0.057
KSrBi	-0.672	0.039	CsBeN	-0.297	0.391
KBaN	<u>0.060</u>	0.432	CsBeP	-0.331	0.206
KBaP	-0.605	0.164	CsBeAs	-0.293	0.128
KBaAs	-0.699	0.084	CsBeSb	-0.101	0.210
KBaSb	-0.695	0.107	CsBeBi	<u>0.034</u>	0.299
KBaBi	-0.622	0.109	CsMgN	-0.237	0.287
RbBeN	-0.365	0.321	CsMgP	-0.622	0.085
RbBeP	-0.341	0.190	CsMgAs	-0.664	0.003
RbBeAs	-0.299	0.110	CsMgSb	-0.583	0.003
RbBeSb	-0.108	0.181	CsMgBi	-0.487	0.003
RbBeBi	<u>0.030</u>	0.270	CsCaN	-0.173	0.366
RbMgN	-0.214	0.308	CsCaP	-0.793	0.090
RbMgP	-0.621	0.086	CsCaAs	-0.865	0.008
RbMgAs	-0.662	0.003	CsCaSb	-0.830	0.007
RbMgSb	-0.576	0.004	CsCaBi	-0.739	0.005
RbMgBi	-0.477	0.003	CsSrN	-0.003	0.418
RbCaN	-0.170	0.367	CsSrP	-0.720	0.085
RbCaP	-0.783	0.091	CsSrAs	-0.809	0.002
RbCaAs	-0.851	0.018	CsSrSb	-0.803	0.003
RbCaSb	-0.807	0.008	CsSrBi	-0.723	0.002
RbCaBi	-0.714	0.007	CsBaN	<u>0.092</u>	0.464
RbSrN	-0.020	0.401	CsBaP	-0.647	0.104
RbSrP	-0.699	0.085	CsBaAs	-0.748	0.023
RbSrAs	-0.784	0.005	CsBaSb	-0.761	0.027
RbSrSb	-0.770	0.012	CsBaBi	-0.691	0.024
RbSrBi	-0.688	0.009			

TABLE S5. Calculated elastic constants C_{11}, C_{12}, C_{13}, C_{33}, C_{44}, and C_{66} for 36 candidate $C^{I}C^{II}A^{V}$ ternary compounds with $\Delta E_{HD} < 50$ meV/atom and crystal structure of Figure 1(d(v)) in the main text. All calculated elastic constants satisfy the Born elastic stability criteria for tetragonal crystals: $C_{11} > |C_{12}|$, $2C_{13}^2 < C_{33}(C_{11} + C_{12})$, $C_{44} > 0$, and $C_{66} > 0$, confirming mechanical stability.

$C_2^I C_3^{II} A_4^{VI}$	C_{11} (GPa)	C_{12} (GPa)	C_{13} (GPa)	C_{33} (GPa)	C_{44} (GPa)	C_{66} (GPa)	stable?
LiBeAs	156.4	5.9	20.5	94.5	12.0	35.6	✓
CsSrAs	34.3	4.3	11.9	28.5	14.4	4.0	✓
CsSrBi	24.1	3.2	3.0	2.5	10.1	4.5	✓
CsMgBi	38.5	4.9	7.7	15.8	16.5	6.9	✓
CsSrSb	28.9	4.1	10.4	23.3	11.2	4.2	✓
RbMgAs	59.2	6.4	8.3	12.3	24.4	11.0	✓
CsMgAs	53.6	6.4	9.0	14.1	25.0	10.4	✓
RbMgBi	42.7	6.7	9.7	22.6	15.6	8.7	✓
CsMgSb	43.6	6.1	8.6	17.3	19.9	7.8	✓
KMgBi	47.6	5.6	10.4	25.9	14.8	10.0	✓
KMgSb	54.2	6.7	12.7	33.1	17.3	11.5	✓
KMgAs	65.8	8.1	14.8	37.8	24.9	14.0	✓
RbMgSb	48.9	6.3	9.5	20.0	18.4	9.7	✓
RbSrAs	34.5	2.4	13.2	28.6	13.2	3.0	✓
CsCaBi	32.1	4.7	10.0	22.0	13.2	5.4	✓
RbCaBi	32.9	4.2	11.0	24.4	12.3	6.1	✓
CsCaSb	35.4	4.9	10.8	23.0	14.4	6.0	✓
CsCaAs	42.7	6.2	12.3	27.0	18.7	6.6	✓
RbCaSb	36.8	4.7	12.8	29.0	13.6	6.3	✓
KCaBi	33.7	3.9	12.0	27.4	11.6	6.2	✓
KCaSb	37.4	4.0	13.6	31.2	12.7	6.4	✓
RbSrBi	26.7	3.0	10.3	22.4	9.4	4.2	✓
KCaAs	45.5	3.7	16.1	36.7	17.1	6.0	✓
RbSrSb	29.4	3.1	11.5	25.1	10.2	4.1	✓
RbCaAs	44.5	4.7	14.4	32.8	17.9	6.7	✓
CsBaAs	24.5	3.7	10.5	25.8	9.4	1.5	✓
CsBaBi	19.4	3.1	8.7	19.3	6.9	2.5	✓
CsBaSb	20.1	3.0	2.4	-1.6	7.1	3.7	✓
NaMgSb	66.9	3.8	14.5	50.8	9.9	13.5	✓
NaMgAs	76.8	5.1	18.8	63.6	17.9	15.8	✓
KSrBi	26.7	2.7	11.0	24.8	8.7	3.2	✓
KSrAs	35.2	0.9	15.1	28.0	12.2	1.2	✓
NaMgBi	58.3	6.8	12.4	42.9	8.0	10.5	✓
KSrSb	28.8	2.5	11.9	26.6	9.2	2.4	✓
LiMgBi	63.4	4.3	11.5	47.2	5.3	9.2	✓
NaBeAs	121.2	18.2	20.7	65.3	22.1	31.2	✓

TABLE S6. Calculated bandgap nature (indirect or direct gap), bandgap value (E_g at DFT/PBE level of theory or DFT/PBE+MBJ level of theory), and average atomic masses (in amu) for 12 highly stable ternary compounds. In all calculations, the spin-orbit interaction is considered.

Materials	Bandgap nature	E_g (PBE) (eV)	E_g (PBE+MBJ+SOC) (eV)	Avg. Atomic Mass (amu)
CsSrAs	Indirect	0.94	2.07	98.48
CsMgBi	Indirect	0.47	1.27	122.07
RbMgAs	Indirect	0.96	2.22	61.57
CsMgAs	Indirect	1.07	2.05	77.38
RbMgBi	Indirect	0.31	0.75	106.25
KMgSb	Indirect	1.26	1.78	61.72
RbMgSb	Indirect	1.08	1.60	77.18
CsCaSb	Indirect	1.60	2.31	98.25
CsCaAs	Indirect	1.44	2.55	82.64
RbCaSb	Indirect	1.48	2.26	82.44
KCaSb	Indirect	1.51	2.17	66.98
RbCaAs	Indirect	1.28	2.51	66.82

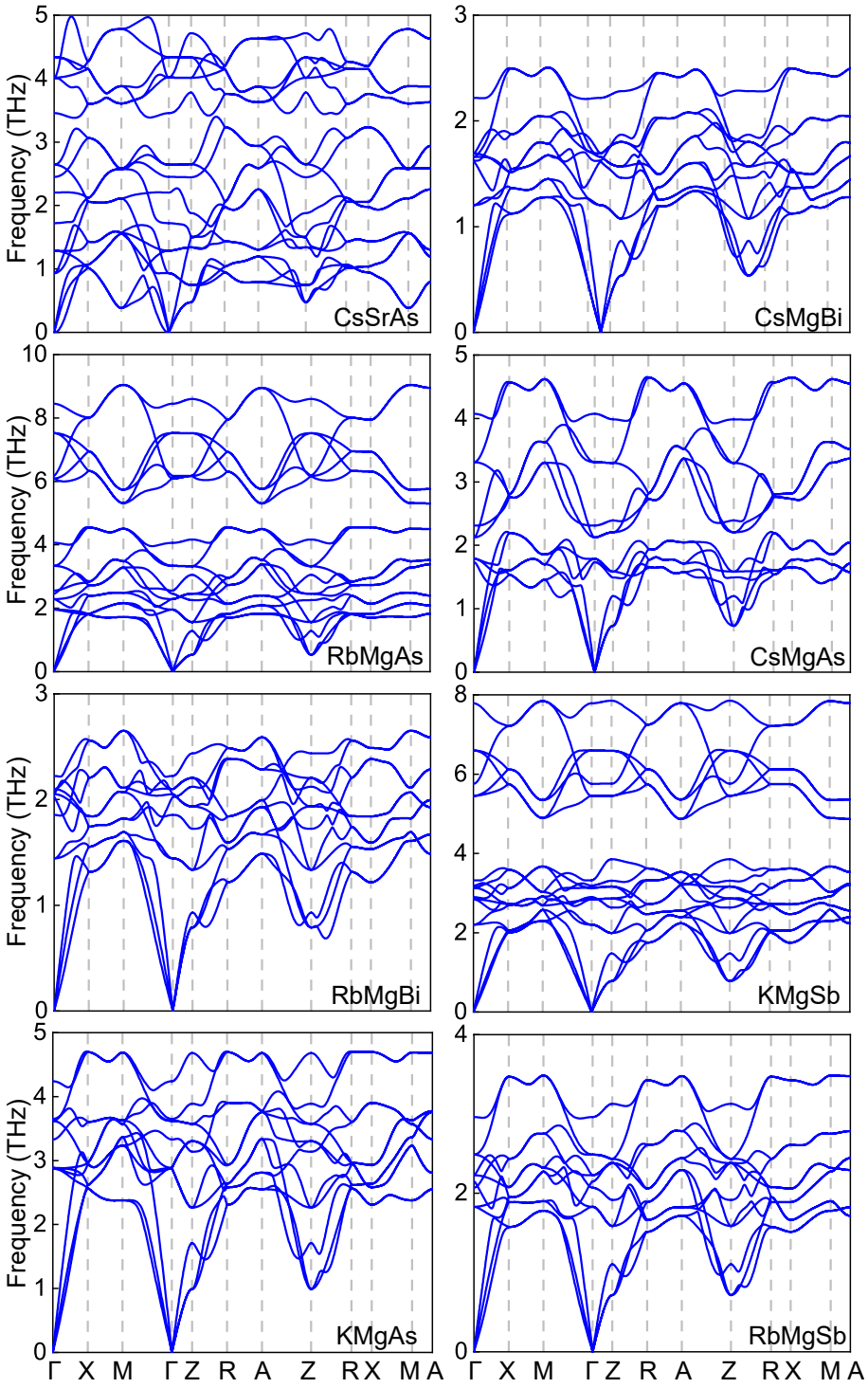

FIG. S1. Calculated phonon spectrum for 8 selected dynamically stable $C^{I}C^{II}A^{V}$ ternary compounds with $\Delta E_{HD} < 50$ meV/atom.

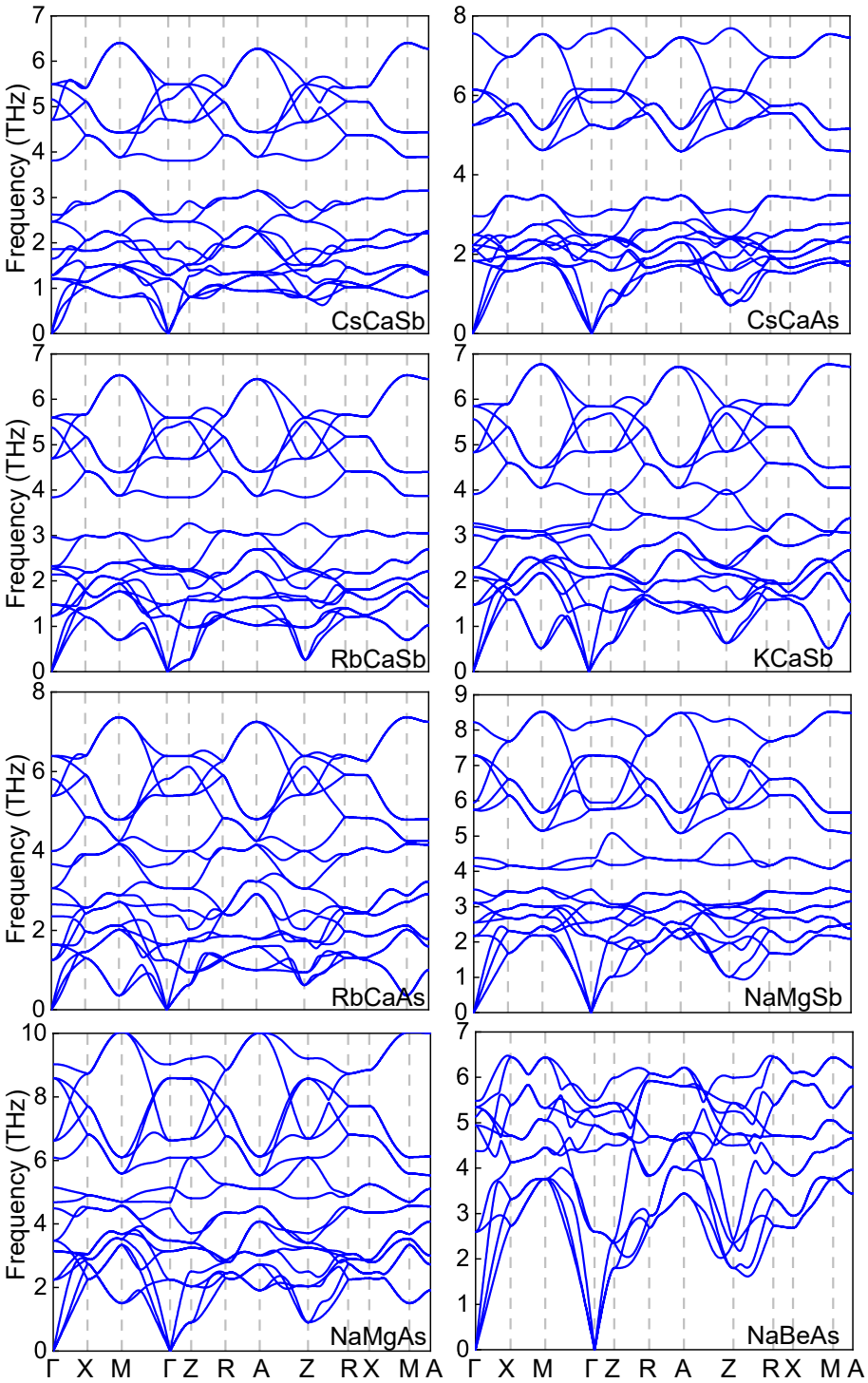

FIG. S2. Calculated phonon spectrum for 8 selected dynamically stable $C^{I}C^{II}A^{V}$ ternary compounds with $\Delta E_{HD} < 50$ meV/atom.

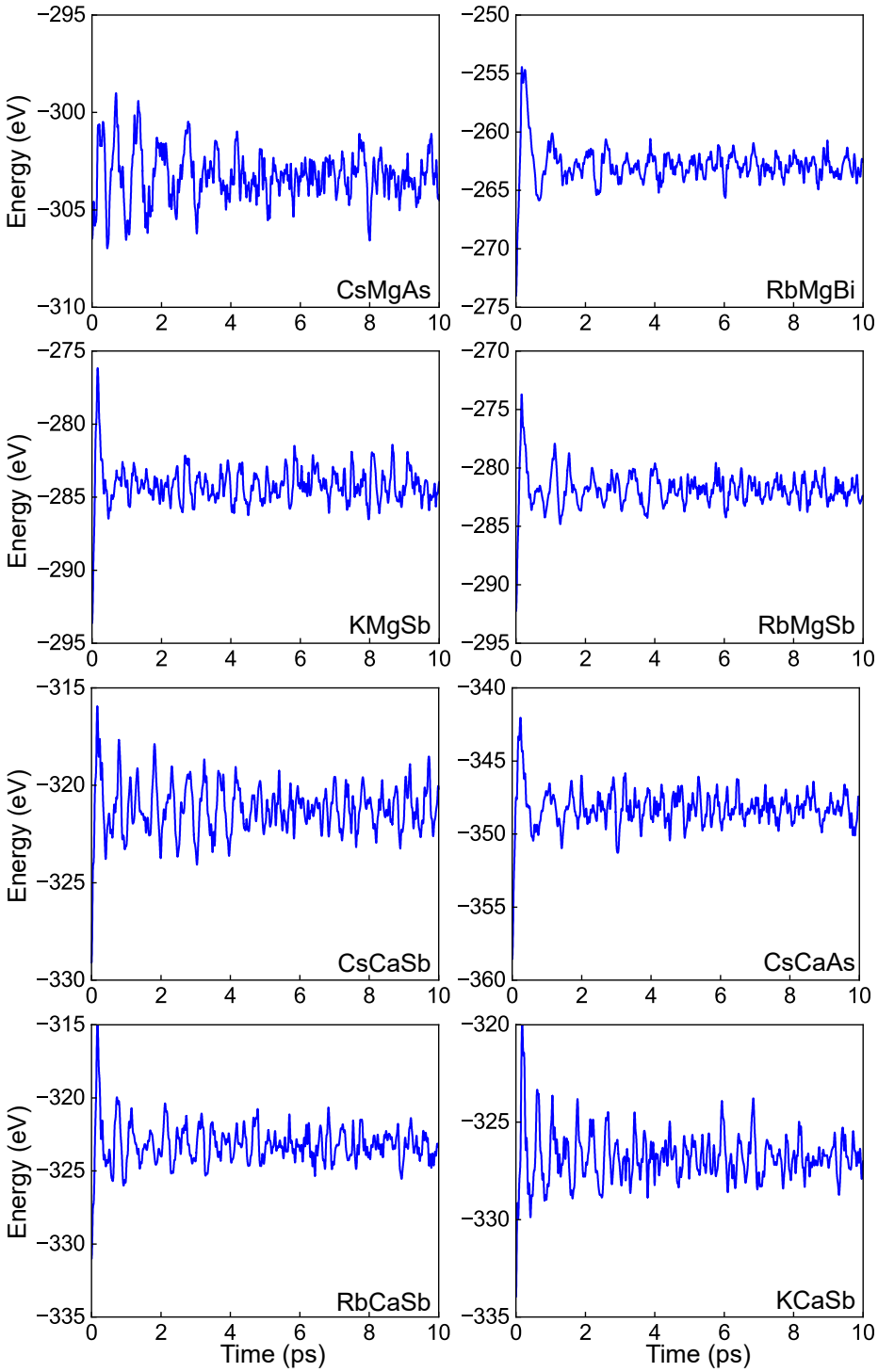

FIG. S3. *ab initio* molecular dynamics (AIMD) simulation of 8 selected thermodynamically stable $C^{I}C^{II}A^{V}$ ternary compounds at the temperature of 800 K for 10 ps.

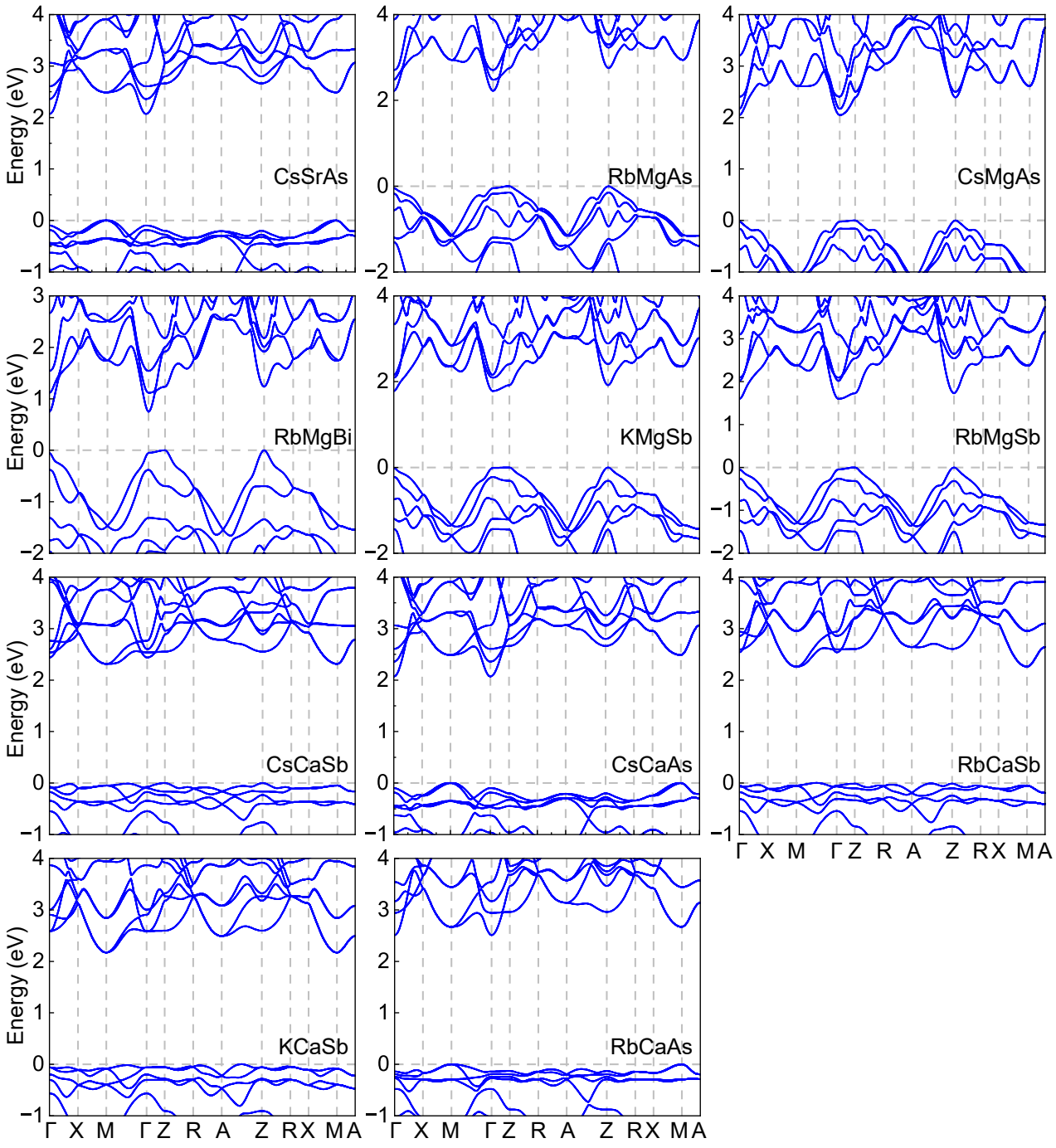

FIG. S4. Electronic band structure for 11 selected highly stable $C^{I}C^{II}A^{V}$ ternary compounds. In all calculations, we use DFT/PBE level of theory and MBJ correction and consider spin-orbit interaction.

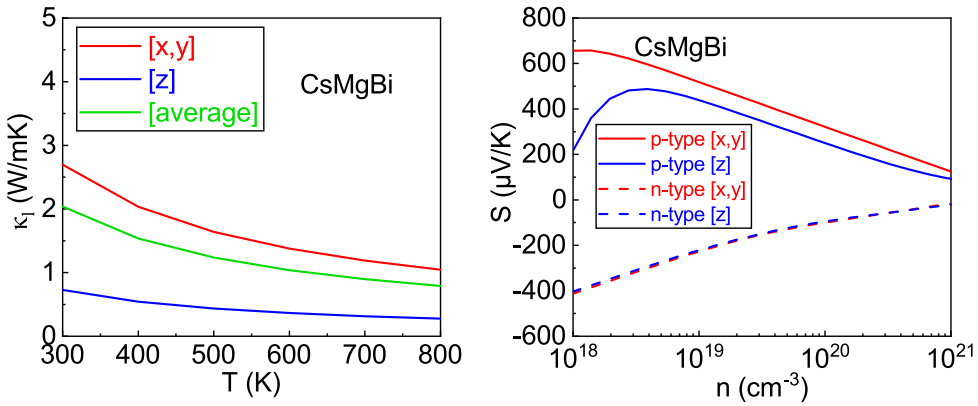

FIG. S5. Lattice thermal conductivity (κ_l) of CsMgBi along different crystallographic axes as a function of temperature (left); Seebeck coefficient (S) of CsMgBi along different crystallographic axes at 800 K for n-type and p-type carriers as a function of carrier density (right).

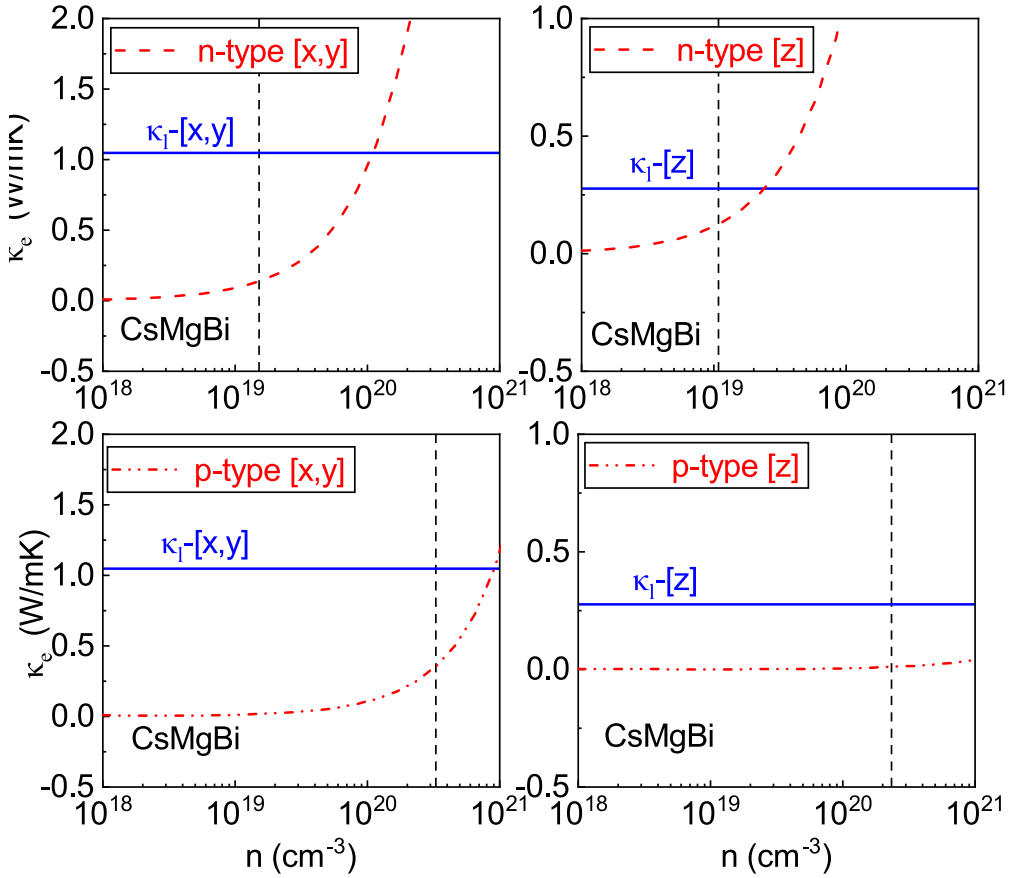

FIG. S6. Electronic thermal conductivity (κ_e) at 800 K for n-type and p-type carriers as a function of carrier density along the different transport directions of CsMgBi. The lattice thermal conductivity (κ_l; blue horizontal solid line) is included for comparison.

TABLE S7. Formation energies E_f (in unit of eV/atom) and hull distance $\Delta E_{\rm HD}$ (in unit of eV/atom) for 35 $C_3^{II}A_2^V$ binary compounds. All the calculations are performed using DFT/PBE level of theory. Those compounds with positive formation energies are underlined.

Materials	E_f (eV/atom)	$\Delta E_{\rm HD}$ (eV/atom)	Materials	E_f (eV/atom)	$\Delta E_{\rm HD}$ (eV/atom)
Be_3N_2	-0.93	0.23	Sr_3Sb_2	-0.84	0.18
Be_3P_2	-0.26	0.08	Sr_3Bi_2	-0.70	0.19
Be_3As_2	-0.08	-0.02	Ba_3N_2	<u>0.01</u>	0.51
Be_3Sb_2	<u>0.30</u>	0.30	Ba_3P_2	-0.78	0.29
Be_3Bi_2	<u>0.58</u>	0.58	Ba_3As_2	-0.87	0.18
Mg_3N_2	-0.46	0.40	Ba_3Sb_2	-0.83	0.18
Mg_3P_2	-0.59	0.19	Ba_3Bi_2	-0.71	0.20
Mg_3As_2	-0.57	0.07	Zn_3N_2	<u>0.34</u>	0.34
Mg_3Sb_2	-0.36	0.02	Zn_3P_2	-0.12	0.17
Mg_3Bi_2	-0.18	0.04	Zn_3As_2	-0.10	0.05
Ca_3N_2	-0.47	0.42	Zn_3Sb_2	<u>0.04</u>	0.07
Ca_3P_2	-0.94	0.31	Zn_3Bi_2	<u>0.18</u>	0.18
Ca_3As_2	-0.98	0.18	Cd_3N_2	<u>0.80</u>	0.80
Ca_3Sb_2	-0.84	0.18	Cd_3P_2	<u>0.04</u>	0.22
Ca_3Bi_2	-0.68	0.18	Cd_3As_2	-0.04	0.07
Sr_3N_2	-0.18	0.44	Cd_3Sb_2	<u>0.01</u>	0.05
Sr_3P_2	-0.85	0.29	Cd_3Bi_2	<u>0.09</u>	0.09
Sr_3As_2	-0.92	0.18			

TABLE S8. Computed elastic constants C_{11}, C_{12}, C_{13}, C_{33}, C_{44} and C_{66} for 18 selected $C_3^{II}A_2^V$ binary compounds with $\Delta E_{\rm HD} < 0.2$ eV/atom. All calculated elastic constants satisfy the Born elastic stability criteria for tetragonal crystals: $C_{11} > |C_{12}|$, $2C_{13}^2 < C_{33}(C_{11}+C_{12})$, $C_{44} > 0$, and $C_{66} > 0$.

Compound	C_{11} (GPa)	C_{12} (GPa)	C_{13} (GPa)	C_{33} (GPa)	C_{44} (GPa)	C_{66} (GPa)	stable?
Be_3As_2	190.7	13.4	45.9	141.2	72.6	38.0	✓
Mg_3Sb_2	73.8	14.1	22.5	59.6	16.9	16.6	✓
Mg_3Bi_2	58.2	14.3	19.8	47.9	5.2	11.7	✓
Mg_3As_2	92.9	21.6	23.8	82.6	22.9	29.0	✓
Be_3P_2	230.3	15.3	47.9	169.8	85.6	53.4	✓
Ba_3As_2	29.9	19.8	11.0	35.7	4.1	12.1	✓
Sr_3Sb_2	34.1	18.0	12.2	36.9	5.3	12.9	✓
Ca_3Bi_2	38.6	18.1	14.0	39.7	4.5	13.3	✓
Ca_3As_2	52.0	27.0	16.0	57.6	9.1	21.7	✓
Ca_3Sb_2	43.4	20.4	15.5	44.8	6.6	15.2	✓
Ba_3Sb_2	25.5	16.0	10.6	29.2	3.7	9.3	✓
Sr_3As_2	40.0	23.2	12.5	46.2	6.8	17.5	✓
Sr_3Bi_2	30.7	16.0	10.9	33.1	3.9	11.5	✓
Mg_3P_2	106.5	27.4	25.6	97.6	27.4	36.6	✓
Ba_3Bi_2	22.8	14.7	9.7	26.6	2.8	8.3	✓
Zn_3As_2	105.1	26.0	42.4	83.2	28.4	17.3	✓
Cd_3As_2	75.2	26.6	32.0	63.6	17.9	14.4	✓
Zn_3P_2	135.6	33.2	44.2	107.9	40.4	26.5	✓

TABLE S9. Calculated bandgap nature, bandgap values at DFT/PBE and DFT/PBE+MBJ+SOC levels of theory (in unit of eV), and average atomic masses (in amu) for 5 stable $C_3^{II}A_2^V$ binary compounds.

Materials	Band nature	E_g(PBE) (eV)	E_g(PBE+MBJ+SOC) (eV)	Avg. Atomic Mass (amu)
Mg_3Sb_2	Indirect	0.47	0.88	60.69
Mg_3As_2	Direct	1.00	1.82	43.68
Be_3P_2	Indirect	0.64	0.94	16.80
Ca_3As_2	Direct	1.49	2.14	52.03
Mg_3P_2	Indirect	1.67	2.35	26.93

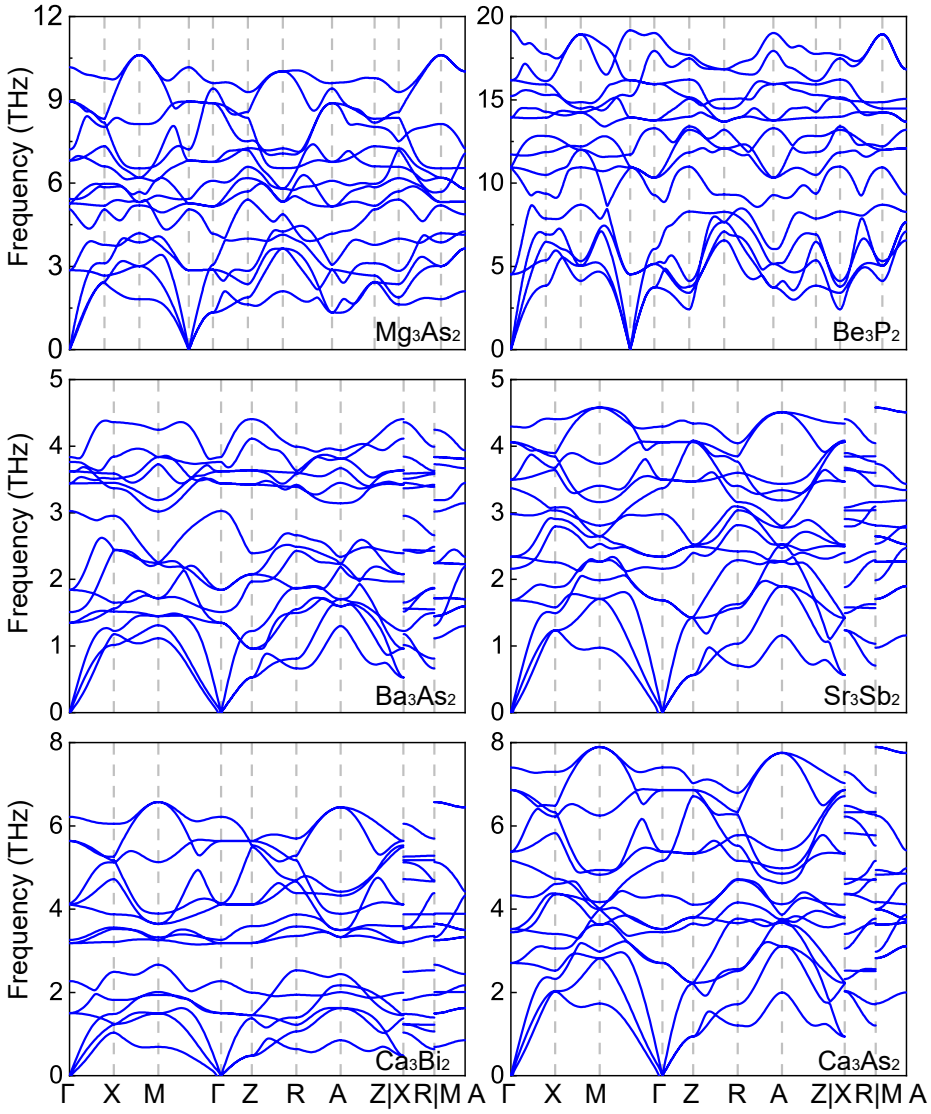

FIG. S7. Calculated phonon spectrum for 6 selected dynamically stable candidates of $C_3^{II}A_2^{V}$ binary compounds with $\Delta E_{HD} < 0.2$ eV/atom.

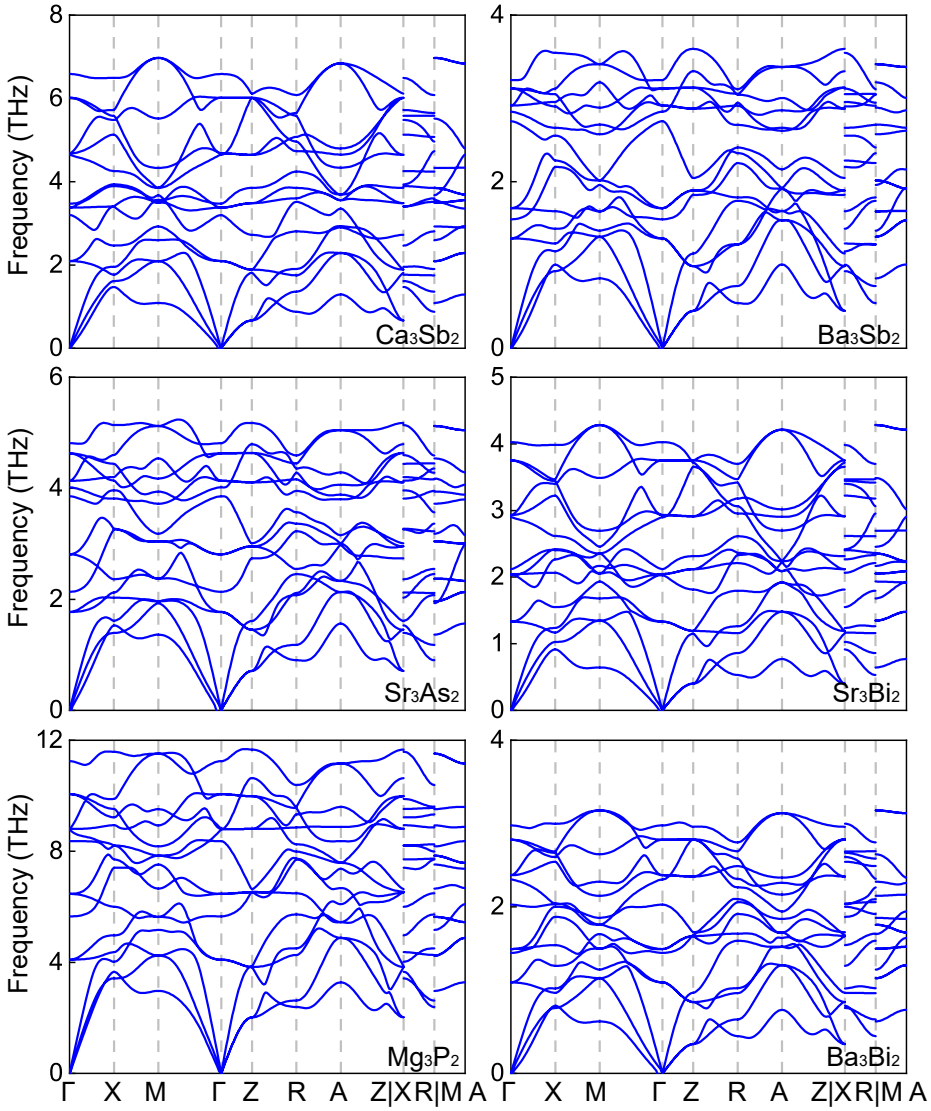

FIG. S8. Calculated phonon spectrum for 6 selected dynamically stable candidates of $C_3^{II}A_2^V$ binary compounds with $\Delta E_{HD} < 0.2$ eV/atom.

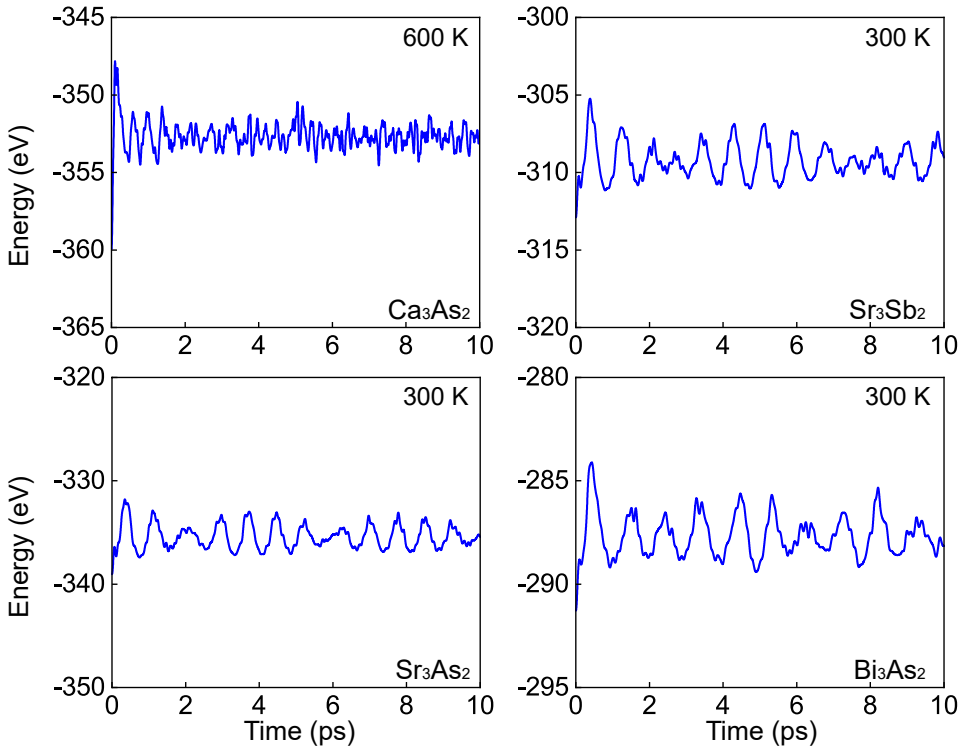

FIG. S9. *ab initio* molecular dynamics (AIMD) simulations of 4 selected $C_3^{II}A_2^V$ binary compounds at lower temperature of 600 K or 300 K for 10 ps.

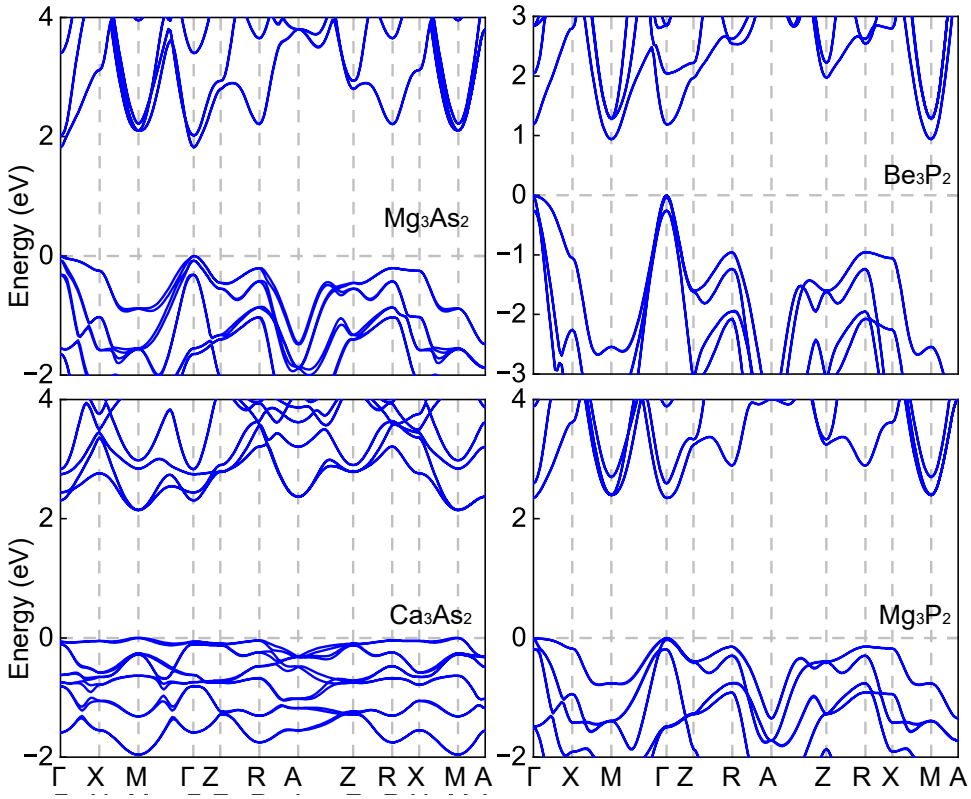

FIG. S10. Electronic band structure for 4 selected $C_3^{II}A_2^V$ binary compounds. All calculations are performed using DFT/PBE level theory and MBJ correction while considering spin-orbit interaction.

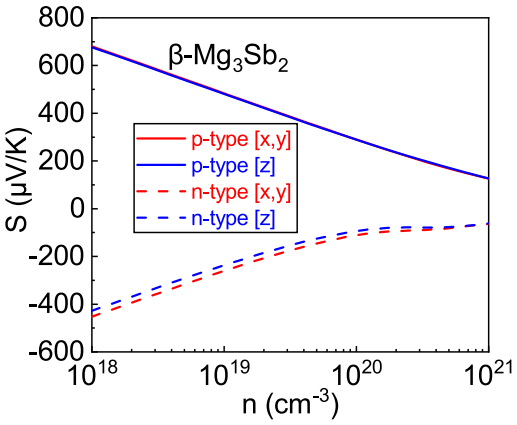

FIG. S11. Seebeck coefficient (S) of β-Mg_3Sb_2 along different crystallographic axes at 800 K for n-type and p-type carriers as a function of carrier density.

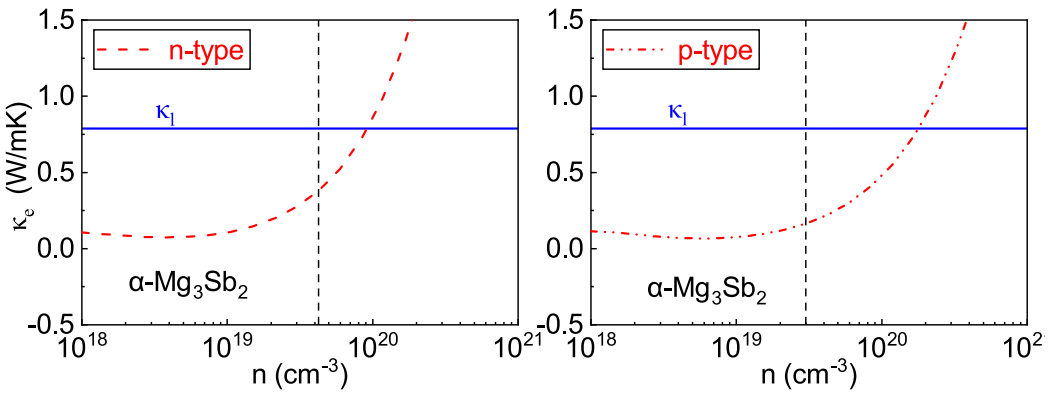

FIG. S12. Electronic thermal conductivity (κ_e) at 800 K for n-type and p-type carriers as a function of carrier density of α-Mg_3Sb_2, with lattice thermal conductivity (κ_l; blue horizontal solid line) shown for comparison.

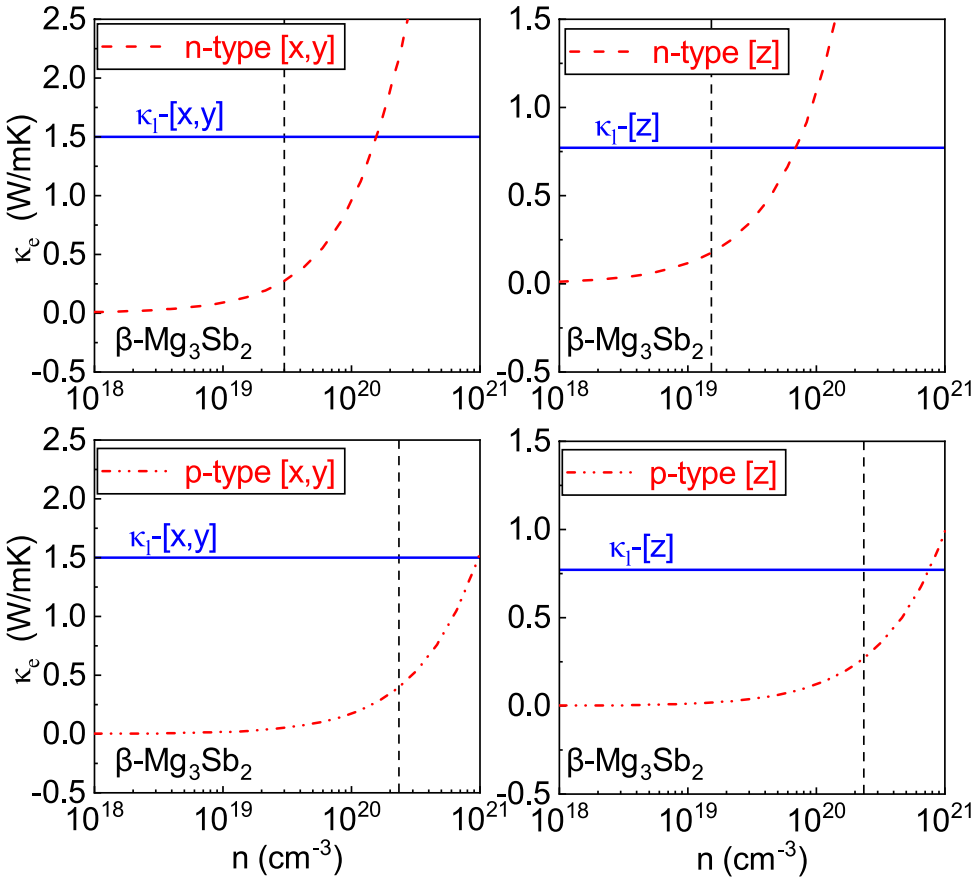

FIG. S13. Electronic thermal conductivity (κ_e) at 800 K for n-type and p-type carriers as a function of carrier density along the different transport directions of β-Mg_3Sb_2, with lattice thermal conductivity (κ_l; blue horizontal solid line) shown for comparison.

TABLE S10. Formation energies E_f (in unit of eV/atom) and hull distance ΔE_{HD} (in unit of eV/atom) for 70 $BeC_2^{II}A_2^{V}$, $MgC_2^{II}A_2^{V}$ and $CaC_2^{II}A_2^{V}$ ternary compounds. All the calculations are performed using DFT/PBE level of theory. Those compounds with positive formation energies are underlined.

Materials	E_f (eV/atom)	ΔE_{HD} (eV/atom)	Materials	E_f (eV/atom)	ΔE_{HD} (eV/atom)
$BeMg_2N_2$	-0.59	0.41	$MgCa_2N_2$	-0.62	0.28
$BeMg_2P_2$	-0.08	0.60	$MgCa_2P_2$	-0.59	0.59
$BeMg_2As_2$	-0.05	0.43	$MgCa_2As_2$	-0.63	0.46
$BeMg_2Sb_2$	<u>0.16</u>	0.41	$MgCa_2Sb_2$	-0.50	0.40
$BeMg_2Bi_2$	<u>0.23</u>	0.38	$MgCa_2Bi_2$	<u>0.99</u>	1.73
$BeCa_2N_2$	-0.53	0.54	$MgSr_2N_2$	-0.35	0.37
$BeCa_2P_2$	-0.51	0.53	$MgSr_2P_2$	-0.54	0.60
$BeCa_2As_2$	-0.50	0.41	$MgSr_2As_2$	-0.60	0.48
$BeCa_2Sb_2$	-0.30	0.44	$MgSr_2Sb_2$	-0.49	0.44
$BeCa_2Bi_2$	<u>0.53</u>	1.16	$MgSr_2Bi_2$	-0.38	0.42
$BeSr_2N_2$	<u>0.06</u>	0.96	$MgBa_2N_2$	-0.14	0.48
$BeSr_2P_2$	-0.39	0.59	$MgBa_2P_2$	-0.60	0.48
$BeSr_2As_2$	-0.41	0.46	$MgBa_2As_2$	-0.58	0.46
$BeSr_2Sb_2$	-0.33	0.44	$MgBa_2Sb_2$	-0.51	0.43
$BeSr_2Bi_2$	<u>0.47</u>	1.14	$MgBa_2Bi_2$	-0.42	0.41
$BeBa_2N_2$	-0.20	0.57	$MgZn_2N_2$	<u>0.45</u>	0.73
$BeBa_2P_2$	-0.53	0.41	$MgZn_2P_2$	-0.23	0.25
$BeBa_2As_2$	-0.36	0.53	$MgZn_2As_2$	-0.21	0.12
$BeBa_2Sb_2$	-0.35	0.45	$MgZn_2Sb_2$	-0.05	0.09
$BeBa_2Bi_2$	-0.22	0.49	$MgZn_2Bi_2$	<u>0.06</u>	0.14
$BeZn_2N_2$	<u>1.27</u>	1.66	$MgCd_2N_2$	<u>0.19</u>	0.48
$BeZn_2P_2$	<u>0.16</u>	0.46	$MgCd_2P_2$	-0.04	0.34
$BeZn_2As_2$	<u>0.19</u>	0.31	$MgCd_2As_2$	-0.11	0.17
$BeZn_2Sb_2$	<u>0.32</u>	0.35	$MgCd_2Sb_2$	-0.04	0.11
$BeZn_2Bi_2$	<u>0.37</u>	0.37	$MgCd_2Bi_2$	<u>0.01</u>	0.08
$BeCd_2N_2$	<u>0.24</u>	0.63	$CaBe_2N_2$	-0.32	0.88
$BeCd_2P_2$	<u>0.28</u>	0.58	$CaBe_2P_2$	-0.70	0.14
$BeCd_2As_2$	<u>0.25</u>	0.34	$CaBe_2As_2$	-0.57	0.05
$BeCd_2Sb_2$	<u>0.33</u>	0.37	$CaBe_2Sb_2$	-0.22	0.16
$BeCd_2Bi_2$	<u>0.31</u>	0.31	$CaBe_2Bi_2$	<u>0.02</u>	0.36
$MgBe_2N_2$	-0.93	0.22	$CaMg_2N_2$	-0.65	0.26
$MgBe_2P_2$	-0.37	0.21	$CaMg_2P_2$	-0.83	0.25
$MgBe_2As_2$	-0.23	0.10	$CaMg_2As_2$	-0.82	0.14
$MgBe_2Sb_2$	<u>0.12</u>	0.24	$CaMg_2Sb_2$	-0.62	0.11
$MgBe_2Bi_2$	<u>0.33</u>	0.41	$CaMg_2Bi_2$	-0.46	0.10

TABLE S11. Formation energies E_f (in unit of eV/atom) and hull distance $\Delta E_{\rm HD}$ (in unit of eV/atom) for 70 $CaC_2^{II}A_2^V$, $SrC_2^{II}A_2^V$ and $BaC_2^{II}A_2^V$ ternary compounds. All the calculations are performed using DFT/PBE level of theory. Those compounds with positive formation energies are underlined.

Materials	E_f (eV/atom)	$\Delta E_{\rm HD}$ (eV/atom)	Materials	E_f (eV/atom)	$\Delta E_{\rm HD}$ (eV/atom)
$CaSr_2N_2$	-0.19	0.52	$SrBa_2N_2$	-0.28	0.27
$CaSr_2P_2$	-0.73	0.47	$SrBa_2P_2$	-0.66	0.43
$CaSr_2As_2$	-0.79	0.35	$SrBa_2As_2$	-0.75	0.31
$CaSr_2Sb_2$	-0.70	0.33	$SrBa_2Sb_2$	-0.71	0.31
$CaSr_2Bi_2$	-0.59	0.30	$SrBa_2Bi_2$	<u>0.62</u>	1.53
$CaBa_2N_2$	-0.30	0.33	$SrZn_2N_2$	-0.11	0.30
$CaBa_2P_2$	-0.64	0.51	$SrZn_2P_2$	-0.63	0.16
$CaBa_2As_2$	-0.73	0.41	$SrZn_2As_2$	-0.61	0.06
$CaBa_2Sb_2$	-0.68	0.36	$SrZn_2Sb_2$	-0.43	0.05
$CaBa_2Bi_2$	-0.58	0.35	$SrZn_2Bi_2$	-0.28	0.10
$CaZn_2N_2$	-0.05	0.42	$SrCd_2N_2$	<u>0.20</u>	0.59
$CaZn_2P_2$	-0.60	0.21	$SrCd_2P_2$	-0.48	0.22
$CaZn_2As_2$	-0.57	0.09	$SrCd_2As_2$	-0.54	0.10
$CaZn_2Sb_2$	-0.39	0.07	$SrCd_2Sb_2$	-0.45	0.08
$CaZn_2Bi_2$	-0.24	0.10	$SrCd_2Bi_2$	-0.34	0.05
$CaCd_2N_2$	<u>0.23</u>	0.63	$BaBe_2N_2$	-0.79	0.25
$CaCd_2P_2$	-0.42	0.25	$BaBe_2P_2$	-0.64	0.16
$CaCd_2As_2$	-0.48	0.13	$BaBe_2As_2$	-0.55	0.06
$CaCd_2Sb_2$	-0.39	0.09	$BaBe_2Sb_2$	-0.25	0.18
$CaCd_2Bi_2$	-0.29	0.06	$BaBe_2Bi_2$	-0.03	0.36
$SrBe_2N_2$	-0.96	0.18	$BaMg_2N_2$	-0.63	0.12
$SrBe_2P_2$	-0.68	0.13	$BaMg_2P_2$	-0.91	0.13
$SrBe_2As_2$	-0.57	0.03	$BaMg_2As_2$	-0.91	0.04
$SrBe_2Sb_2$	-0.24	0.16	$BaMg_2Sb_2$	-0.73	0.04
$SrBe_2Bi_2$	-0.01	0.35	$BaMg_2Bi_2$	-0.58	0.05
$SrMg_2N_2$	-0.65	0.15	$BaCa_2N_2$	-0.49	0.27
$SrMg_2P_2$	-0.88	0.19	$BaCa_2P_2$	-1.01	0.22
$SrMg_2As_2$	-0.88	0.09	$BaCa_2As_2$	-1.06	0.13
$SrMg_2Sb_2$	-0.68	0.08	$BaCa_2Sb_2$	-0.95	0.12
$SrMg_2Bi_2$	-0.53	0.08	$BaCa_2Bi_2$	-0.81	0.12
$SrCa_2N_2$	-0.47	0.33	$BaSr_2N_2$	-0.22	0.37
$SrCa_2P_2$	-0.95	0.29	$BaSr_2P_2$	-0.80	0.32
$SrCa_2As_2$	-1.00	0.19	$BaSr_2As_2$	-0.87	0.21
$SrCa_2Sb_2$	-0.88	0.17	$BaSr_2Sb_2$	-0.87	0.15
$SrCa_2Bi_2$	-0.74	0.14	$BaSr_2Bi_2$	-0.75	0.15

TABLE S12. Formation energies E_f (in unit of eV/atom) and hull distance $\Delta E_{\rm HD}$ (in unit of eV/atom) for 70 $BaC_2^{II}A_2^V$, $ZnC_2^{II}A_2^V$ and $CdC_2^{II}A_2^V$ ternary compounds. All the calculations are performed using DFT/PBE level of theory. Those compounds with positive formation energies are underlined.

Materials	E_f (eV/atom)	$\Delta E_{\rm HD}$ (eV/atom)	Materials	E_f (eV/atom)	$\Delta E_{\rm HD}$ (eV/atom)
$BaZn_2N_2$	-0.10	0.32	$ZnCd_2N_2$	<u>0.49</u>	0.49
$BaZn_2P_2$	-0.63	0.14	$ZnCd_2P_2$	<u>0.17</u>	0.42
$BaZn_2As_2$	-0.63	0.05	$ZnCd_2As_2$	<u>0.10</u>	0.22
$BaZn_2Sb_2$	-0.47	0.07	$ZnCd_2Sb_2$	<u>0.11</u>	0.15
$BaZn_2Bi_2$	-0.33	0.08	$ZnCd_2Bi_2$	<u>0.12</u>	0.12
$BaCd_2N_2$	<u>0.20</u>	0.60	$CdBe_2N_2$	<u>0.55</u>	1.32
$BaCd_2P_2$	-0.52	0.17	$CdBe_2P_2$	-0.09	0.22
$BaCd_2As_2$	-0.58	0.07	$CdBe_2As_2$	0.00	0.07
$BaCd_2Sb_2$	<u>0.11</u>	0.67	$CdBe_2Sb_2$	<u>0.23</u>	0.25
$BaCd_2Bi_2$	-0.38	0.06	$CdBe_2Bi_2$	<u>0.34</u>	0.34
$ZnBe_2N_2$	-0.48	0.29	$CdMg_2N_2$	-0.07	0.51
$ZnBe_2P_2$	-0.07	0.25	$CdMg_2P_2$	-0.25	0.33
$ZnBe_2As_2$	<u>0.03</u>	0.13	$CdMg_2As_2$	-0.27	0.19
$ZnBe_2Sb_2$	<u>0.27</u>	0.30	$CdMg_2Sb_2$	-0.13	0.14
$ZnBe_2Bi_2$	<u>0.43</u>	0.43	$CdMg_2Bi_2$	-0.05	0.10
$ZnMg_2N_2$	-0.41	0.17	$CdCa_2N_2$	-0.36	0.30
$ZnMg_2P_2$	-0.19	0.43	$CdCa_2P_2$	-0.51	0.51
$ZnMg_2As_2$	-0.20	0.28	$CdCa_2As_2$	-0.58	0.37
$ZnMg_2Sb_2$	-0.07	0.19	$CdCa_2Sb_2$	-0.48	0.33
$ZnMg_2Bi_2$	-0.01	0.14	$CdCa_2Bi_2$	-0.38	0.30
$ZnCa_2N_2$	-0.42	0.38	$CdSr_2N_2$	-0.15	0.40
$ZnCa_2P_2$	-0.55	0.55	$CdSr_2P_2$	-0.49	0.52
$ZnCa_2As_2$	-0.53	0.48	$CdSr_2As_2$	-0.54	0.43
$ZnCa_2Sb_2$	-0.43	0.38	$CdSr_2Sb_2$	-0.47	0.38
$ZnCa_2Bi_2$	-0.30	0.37	$CdSr_2Bi_2$	-0.38	0.36
$ZnSr_2N_2$	<u>0.14</u>	0.78	$CdBa_2N_2$	<u>0.03</u>	0.55
$ZnSr_2P_2$	-0.41	0.63	$CdBa_2P_2$	-0.46	0.51
$ZnSr_2As_2$	-0.48	0.49	$CdBa_2As_2$	-0.55	0.40
$ZnSr_2Sb_2$	<u>0.02</u>	0.86	$CdBa_2Sb_2$	-0.45	0.44
$ZnSr_2Bi_2$	<u>0.07</u>	0.76	$CdBa_2Bi_2$	-0.40	0.38
$ZnBa_2N_2$	-0.07	0.43	$CdZn_2N_2$	<u>0.72</u>	0.72
$ZnBa_2P_2$	-0.62	0.37	$CdZn_2P_2$	0.00	0.27
$ZnBa_2As_2$	<u>0.09</u>	1.04	$CdZn_2As_2$	-0.03	0.10
$ZnBa_2Sb_2$	-0.41	0.47	$CdZn_2Sb_2$	<u>0.05</u>	0.08
$ZnBa_2Bi_2$	-0.36	0.40	$CdZn_2Bi_2$	<u>0.11</u>	0.11

TABLE S13. Computed elastic constants C_{11}, C_{22}, C_{33}, C_{44}, C_{55} , C_{66} , C_{12} , C_{13} and C_{23} for 31 selected $C^{II}C_2^{II}A_2^{V}$ ternary compounds.

$C^{I}C_2^{II}A_2^{VI}$	C_{11} (GPa)	C_{22} (GPa)	C_{33} (GPa)	C_{44} (GPa)	C_{55} (GPa)	C_{66} (GPa)	C_{12} (GPa)	C_{13} (GPa)	C_{23} (GPa)	stable?
$SrBe_2As_2$	123.8	147.1	93.8	40.6	1.7	21.2	13.0	28.9	37.6	✓
$BaMg_2As_2$	80.4	97.0	62.2	26.6	4.2	23.4	12.1	21.4	23.7	✓
$BaMg_2Sb_2$	65.8	76.8	46.0	22.2	3.6	15.5	10.3	16.9	21.0	✓
$BaMg_2Bi_2$	57.0	67.1	39.2	18.9	0.6	12.2	8.7	14.8	18.6	✓
$CaBe_2As_2$	141.6	161.0	96.5	36.0	16.2	19.5	12.0	29.1	37.3	✓
$BaZn_2As_2$	90.9	103.3	66.6	27.9	1.9	18.2	15.9	24.4	31.9	✓
$SrZn_2As_2$	104.0	117.5	68.7	26.2	11.4	16.1	15.5	23.9	32.0	✓
$BaCd_2As_2$	82.7	96.3	58.9	24.9	4.2	16.1	16.3	21.3	27.4	✓
$SrMg_2Bi_2$	62.2	72.3	40.3	17.9	5.2	12.8	9.4	16.1	19.3	✓
$SrMg_2Sb_2$	70.5	83.3	49.1	20.2	8.4	14.5	10.3	17.4	21.3	✓
$CaCd_2Sb_2$	75.6	78.9	46.1	12.4	17.9	8.3	18.5	20.7	28.0	✓
$SrMg_2As_2$	86.6	104.6	65.8	22.9	10.3	22.7	11.5	20.9	22.9	✓
$CaZn_2As_2$	118.3	128.1	72.4	22.3	21.5	14.2	15.9	25.3	31.5	✓
$CaMg_2Bi_2$	65.1	75.8	44.8	13.6	12.9	10.9	10.6	17.9	18.8	✓
$SrCd_2As_2$	92.7	104.7	60.9	22.2	9.0	15.1	16.1	22.0	26.6	✓
$SrZn_2Sb_2$	72.0	78.3	41.7	14.7	11.1	12.7	20.6	20.9	31.3	✓
$CaCd_2Bi_2$	59.1	62.3	46.6	9.8	12.1	8.1	20.5	25.6	26.6	✓
$BaCd_2Bi_2$	47.3	60.1	34.8	10.9	4.3	7.4	15.9	14.0	21.4	✓
$BaZn_2Sb_2$	64.5	77.3	45.6	15.9	6.8	12.2	19.2	20.0	31.1	✓
$CaZn_2Sb_2$	81.1	81.9	45.3	9.7	11.3	10.3	22.7	22.8	29.8	✓
$SrCd_2Sb_2$	73.4	77.0	41.9	15.6	13.1	11.4	15.5	19.0	26.3	✓
$BaZn_2Bi_2$	50.0	55.9	33.5	15.4	6.0	15.9	15.2	17.2	28.4	✓
$CdMg_2Bi_2$	54.6	42.7	41.0	9.4	16.6	11.4	33.6	13.7	29.0	✓
$SrZn_2Bi_2$	56.8	50.0	37.2	10.3	8.3	13.8	18.0	22.1	29.2	✓
$CaZn_2Bi_2$	58.9	54.7	43.4	4.2	10.0	10.2	22.1	22.3	33.2	✓
$CdZn_2As_2$	84.1	89.9	70.1	-1.5	20.4	0.4	34.0	30.1	37.6	×
$SrCd_2Bi_2$	59.1	60.4	38.4	12.7	-7.0	11.0	17.8	20.1	27.3	×
$CdBe_2As_2$	70.2	85.9	81.8	-46.6	27.2	-16.2	66.5	56.9	28.8	×
$MgZn_2Sb_2$	49.9	63.1	51.0	3.6	17.7	-4.8	42.8	23.7	32.0	×
$MgBe_2As_2$	138.2	151.2	112.3	-11.8	41.7	-10.6	21.9	29.7	42.9	×
$BaBe_2As_2$	106.8	125.7	91.5	42.7	-13.9	22.3	15.3	29.1	39.0	×

TABLE S14. Calculated bandgap nature, bandgap values obtained at DFT/PBE and DFT/PBE+MBJ+SOC levels of theory (in unit of eV), and average atomic masses (in amu) for 9 highly stable compounds.

Materials	Band nature	E_g(PBE) (eV)	E_g(PBE+MBJ+SOC) (eV)	Avg. Atomic Mass (amu)
$CaBe_2As_2$	Indirect	0.69	1.10	41.59
$BaZn_2As_2$	Indirect	-0.03	0.72	83.59
$SrZn_2As_2$	Indirect	0.33	1.03	73.64
$BaCd_2As_2$	Indirect	0.48	1.05	102.40
$SrMg_2Bi_2$	Indirect	0.52	0.67	110.84
$SrMg_2Sb_2$	Indirect	1.01	1.23	76.15
$CaZn_2As_2$	Indirect	0.50	1.10	64.14
$CaMg_2Bi_2$	Indirect	0.39	0.51	101.33
$SrCd_2As_2$	Direct	0.39	1.14	92.46

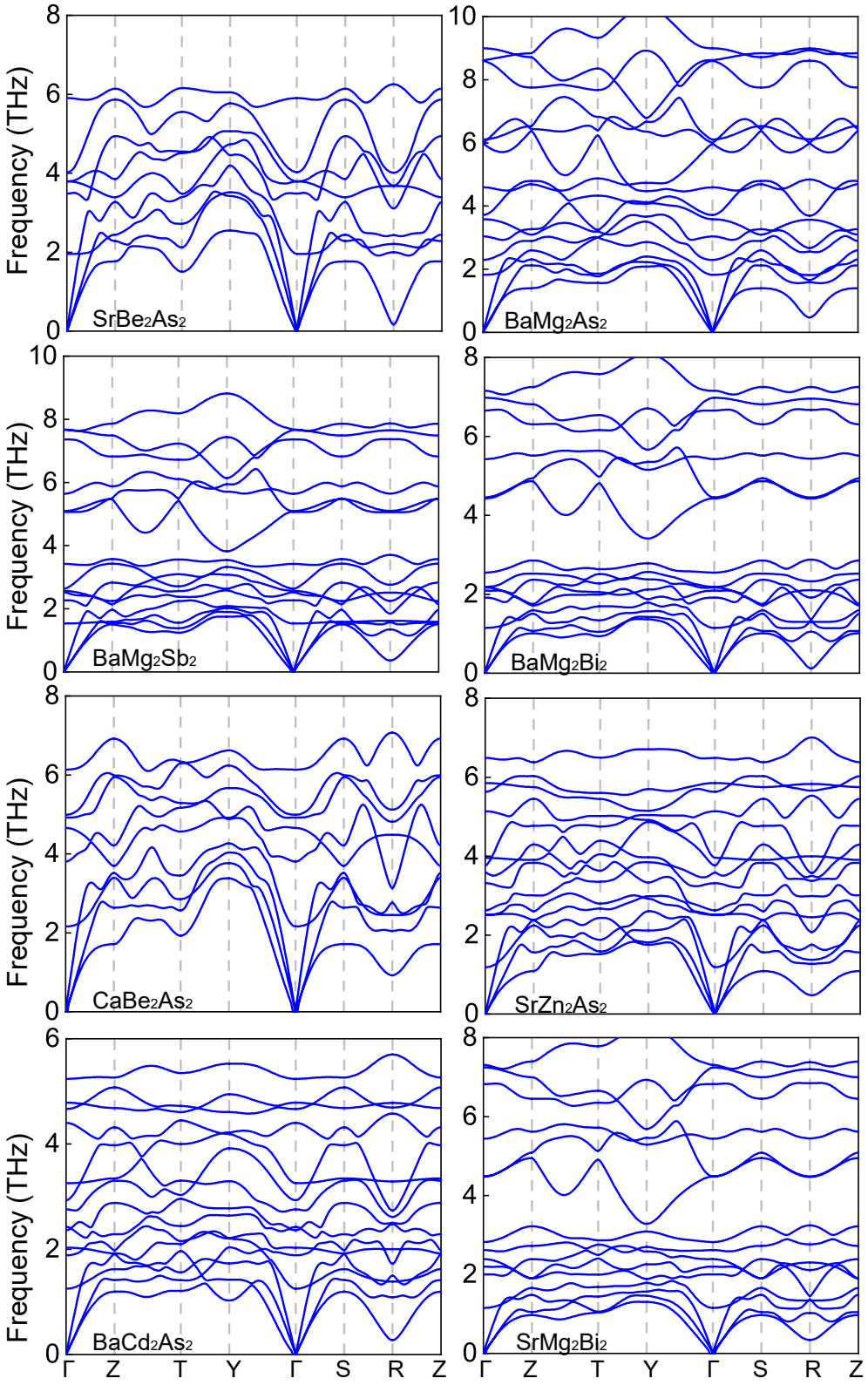

FIG. S14. Calculated phonon spectrum for 8 selected $C^{II}C_2^{II}A_2^{V}$ ternary compounds.

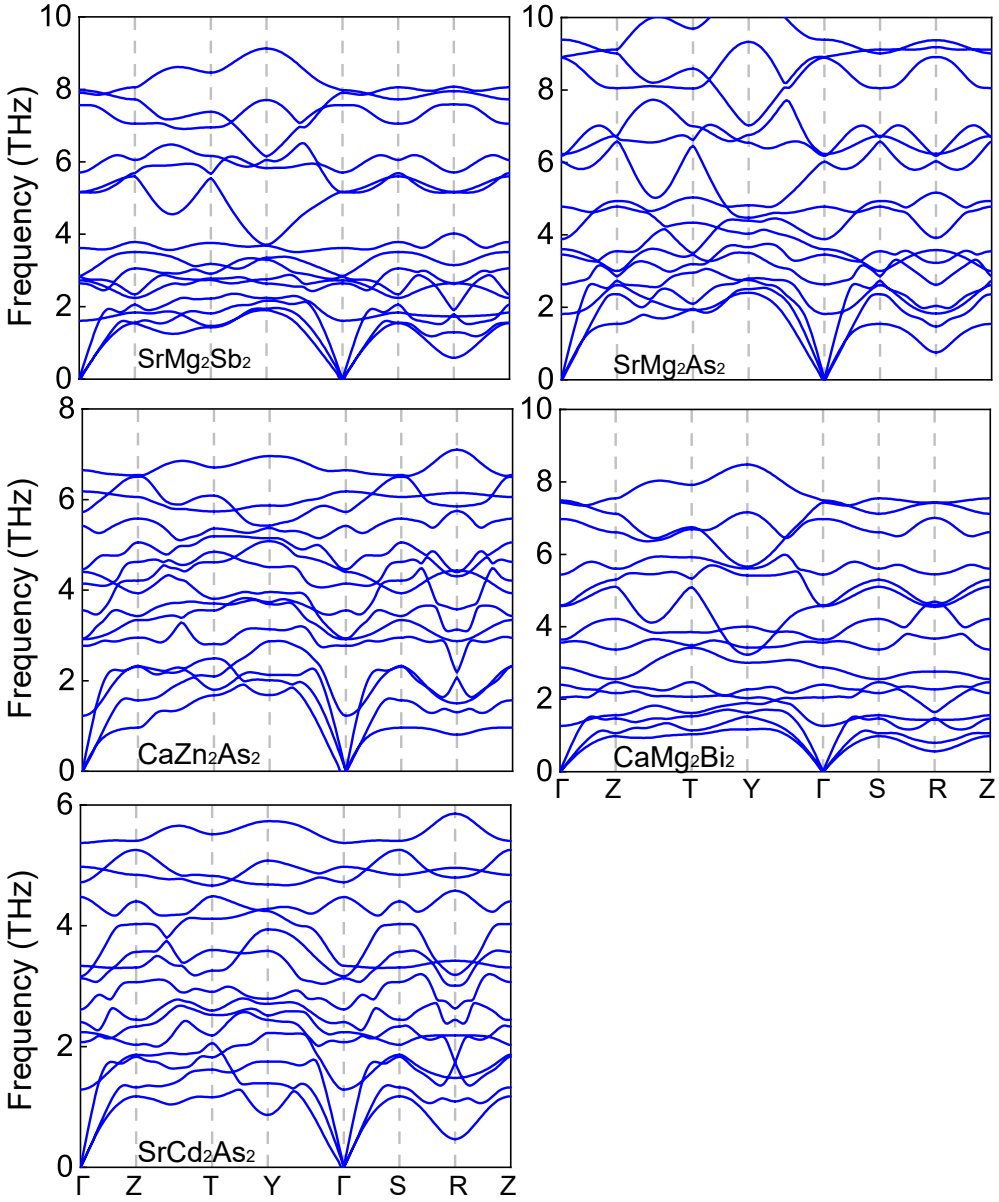

FIG. S15. Calculated phonon spectrum for 5 selected $C^{II}C_2^{II}A_2^{V}$ ternary compounds.

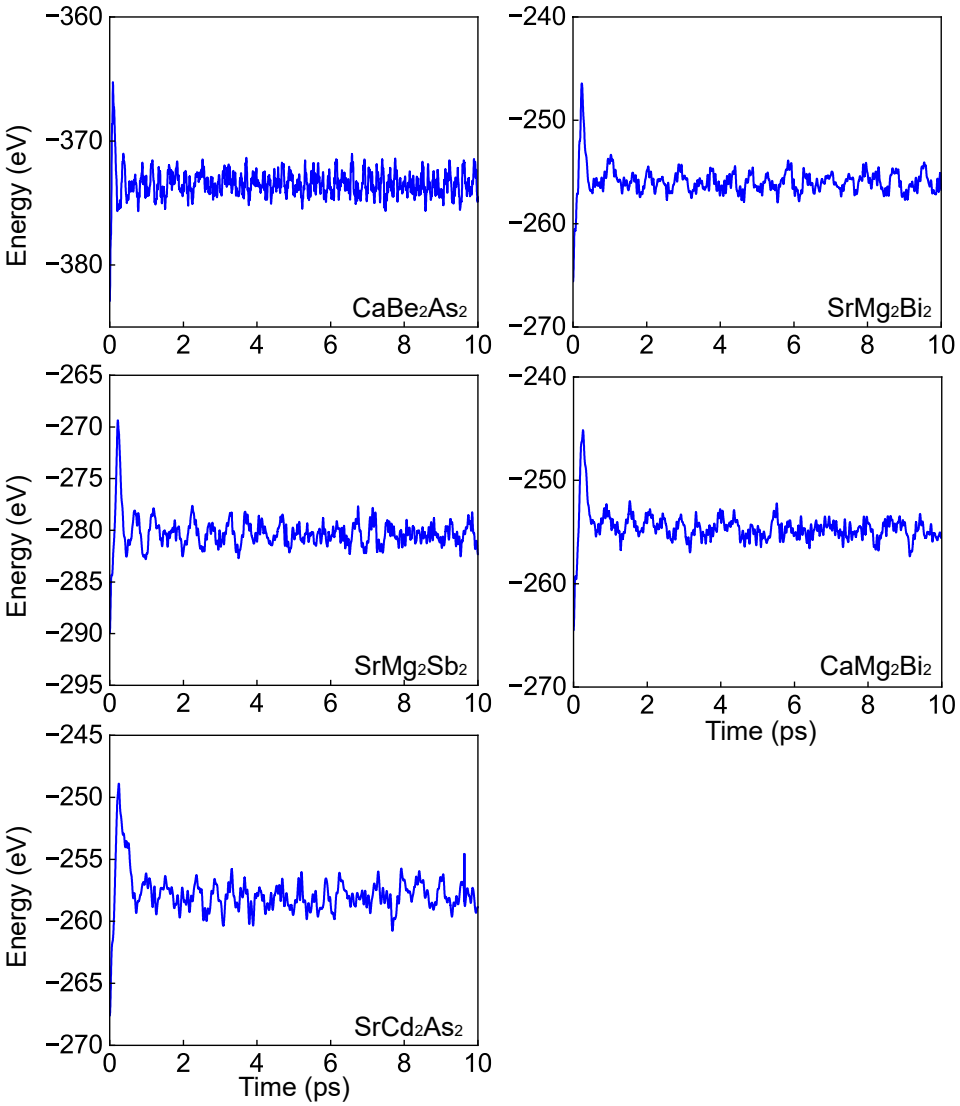

FIG. S16. *ab initio* molecular dynamics (AIMD) simulation of 5 selected $C^{II}C_2^{II}A_2^{V}$ ternary compounds at the temperature of 800 K for 10 ps.

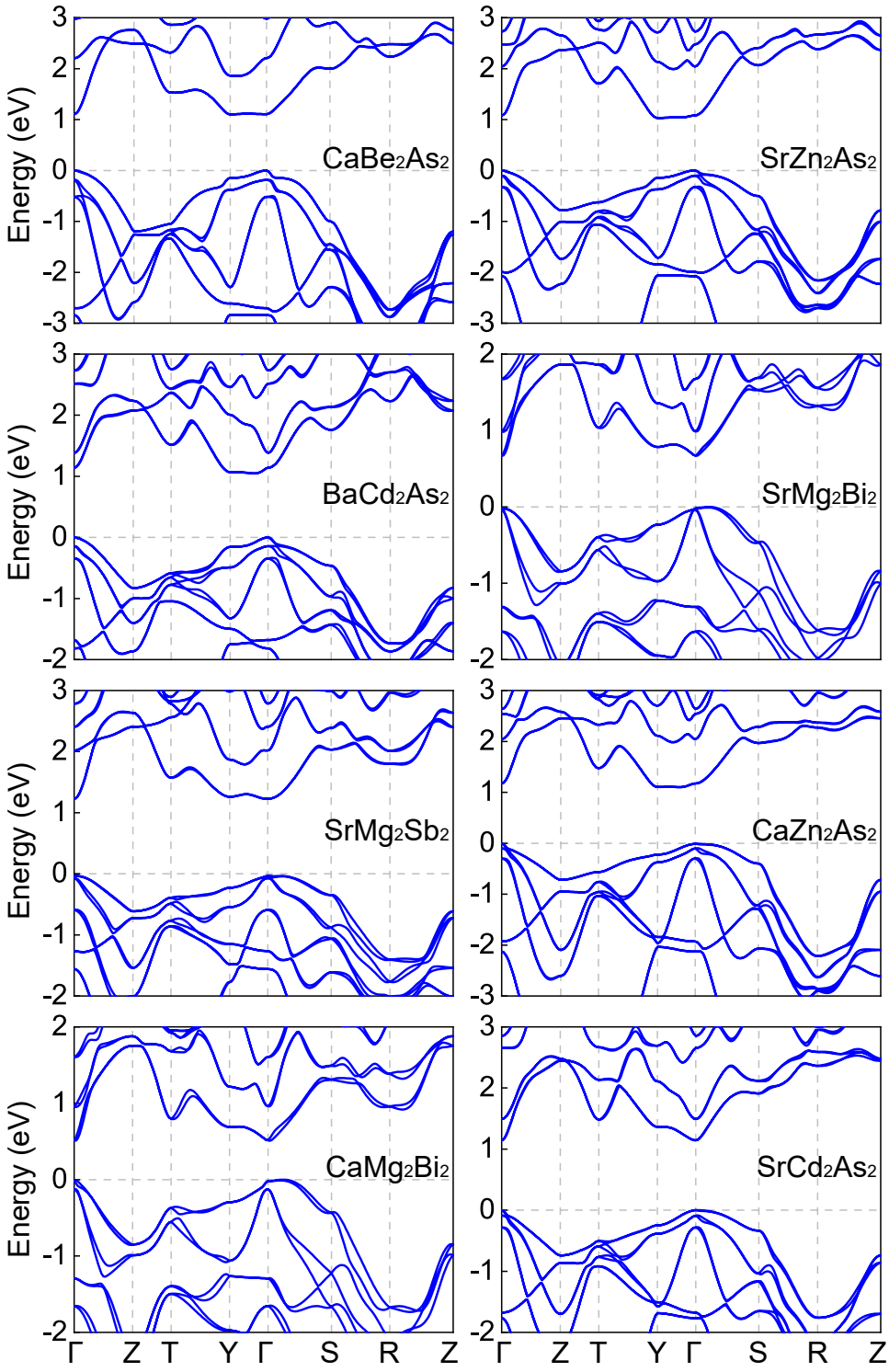

FIG. S17. Calculated Electronic band structure for 8 selected stable $C^{II}C_2^{II}A_2^{V}$ ternary compounds. All calculations are performed using DFT/PBE level theory and MBJ correction while considering spin-orbit interaction.

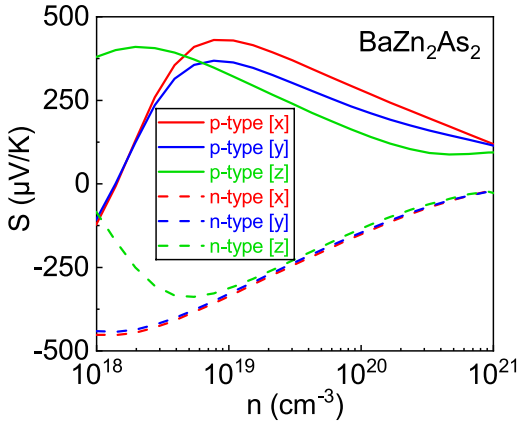

FIG. S18. Seebeck coefficient (S) of $BaZn_2As_2$ along different crystallographic axes at 800 K for n-type and p-type carriers as a function of carrier density.